

# Crystal and Molecular Structure of Pyrrole-2-carboxylic Acid; $\pi$ -Electron Delocalization of Its Dimers—DFT and MP2 Calculations

Sławomir J. Grabowski,<sup>\*,†,‡</sup> Alina T. Dubis,<sup>§</sup> Dariusz Martynowski,<sup>||</sup> Marek Główa,<sup>||</sup> Marcin Palusiak,<sup>†</sup> and Jerzy Leszczynski<sup>‡</sup>

Department of Crystallography and Crystal Chemistry, University of Łódź, ul. Pomorska 149/153, 90-236 Łódź, Poland, Computational Center for Molecular Structure and Interactions, Department of Chemistry, Jackson State University, Jackson, Mississippi 39217, Institute of Chemistry, University of Białystok, Al. J. Piłsudskiego 11/4, 15-443 Białystok, Poland, and Department of X-ray and Chemical Crystallography, Institute of General and Ecological Chemistry, Technical University of Łódź, ul. Zwirki 36, 90-924 Łódź, Poland

Received: November 4, 2003; In Final Form: April 18, 2004

The crystal and molecular structure of pyrrole-2-carboxylic acid (PCA) determined by single-crystal X-ray diffraction is presented. Intermolecular H-bonds for this structure are analyzed. The DFT calculations at the B3LYP/6-311++G(d,p) level of theory and ab initio calculations at the MP2/6-311++G(d,p) level are performed for dimers of pyrrole-2-carboxylic acid and for similar model species. The X-ray data and calculations show that the pyrrole moiety within pyrrole-2-carboxylic acid influences the  $\pi$ -electron delocalization and hence the strength of the hydrogen bonds. The geometrical and energetic features of H-bonds of PCA dimers and of model complexes are analyzed. Additionally, the Bader theory is applied, and the characteristics of the bond critical points and ring critical points confirm the influence of the pyrrole moiety on the strength of H-bond interactions.

## Introduction

Among different hydrogen bonds, the O—H $\cdots$ O and N—H $\cdots$ O bonds most often occur in the gas phase, in liquids, and in crystals.<sup>1,2</sup> They play a crucial role in biological systems such as proteins and DNA base pairs and are essential for life processes.<sup>1</sup> They also strongly influence the arrangement of molecules in crystals and are well known as a driving force able to govern crystal packings.<sup>3,4</sup> Hence, a lot of studies deal with these interactions to explain their nature, strength, and other features important for physical, chemical, and biochemical processes such as the proton-transfer reaction, phase transitions, molecular association in solution, etc.<sup>4,5</sup>

A variety of factors may influence the features of H-bonds; among them,  $\pi$ -electron delocalization within H-bonded systems is very important.<sup>6</sup> The well-known resonance-assisted hydrogen bonds (RAHBs) are an example of  $\pi$ -electron delocalized systems and are often investigated.<sup>7–9</sup> For such interactions, the neutral donor and acceptor atoms are connected through  $\pi$ -conjugated double bonds.<sup>7a</sup> The malonaldehyde molecule is a simple example of intramolecular RAHB that is often investigated (see Chart 1).<sup>10</sup>

For this moiety and all related RAHB systems containing the O=C(R<sub>1</sub>)—C(R<sub>2</sub>)=C(R<sub>3</sub>)—O(H) chain, the equalization of C—C, C=C and C—O, C=O pairs of bond lengths is observed.<sup>7a,10</sup> It was pointed out that the greater is the  $\pi$ -electron delocalization the stronger are the hydrogen bonds. The  $\pi$ -electron delocalization is greater for the electron-withdrawing R<sub>1</sub> substituents and for the electron-donating R<sub>3</sub> substituents

CHART 1: Scheme of the Malonaldehyde Molecule

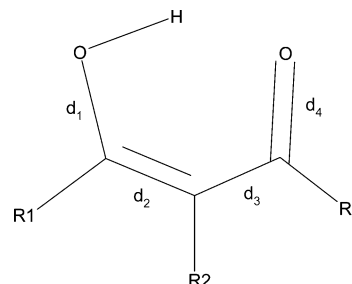


(Chart 1).<sup>7b</sup> This statement has since been confirmed theoretically for malonaldehyde and its simple fluorine and chlorine derivatives. The ab initio calculations performed at the MP2/6-311++G(d,p) level have shown that the greatest equalization of the CC and CO bonds and the greatest strength of the H-bonds are for the chlorine and fluorine atoms substituted at the R<sub>1</sub> position; the weakest H-bonds and the slightest bond equalizations are for these atoms at the R<sub>3</sub> position. Additionally, good correlation between the H-bond strength descriptors was revealed.<sup>10</sup>

There are also other kinds of intramolecular RAHBs such as those involving N—H $\cdots$ O, O—H $\cdots$ N, O—H $\cdots$ S, etc., which were investigated both experimentally<sup>6</sup> and theoretically.<sup>9,11</sup> For example, it was found for the crystal structures of chromone derivatives<sup>6</sup> that N—H $\cdots$ O or O—H $\cdots$ N intramolecular RAHBs exist. The existence of N—H $\cdots$ O bonds is common for chromone derivatives,<sup>12</sup> while O—H $\cdots$ N bonds are very scarce. Very recently, the crystal structure of (*E*)-3-[[diphenoxyphosphoryl]-2-methylhydrazone]-methylene]-4-hydroxy-2*H*-1-benzopyran-2-one was investigated using the X-ray diffraction technique, and it is the only pyrane derivative reported for which intramolecular O—H $\cdots$ N bonds exist.<sup>6</sup> The same study consid-

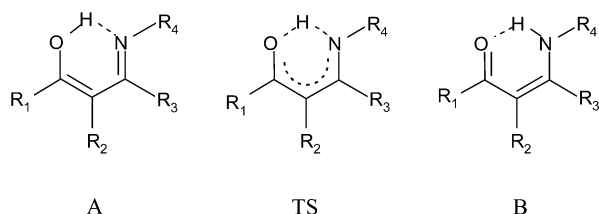
\* Corresponding author. E-mail: slagra@ccmsi.us.

<sup>†</sup> University of Łódź.

<sup>‡</sup> Jackson State University.

<sup>§</sup> University of Białystok.

<sup>||</sup> Technical University of Łódź.

**CHART 2: Tautomeric Forms (A and B) for the Simple Enaminones and the Transition State (TS)**

ered theoretically the proton-transfer reaction for simple model species (Chart 2) and the equilibrium between the enol and enamine forms (at the MP2/6-311++G(d,p) and MP4/6-311++G(d,p) levels). It was shown (Chart 2) that the B form is more stable than the A form and that the potential barrier height for the proton-transfer reaction  $\text{N}-\text{H}\cdots\text{O}=\rightleftharpoons\text{N}\cdots\text{H}-\text{O}$  strongly depends on the  $\text{R}_4$  substituent.<sup>6</sup> It is in line with the study on keto-hydrazone-azo-enol systems<sup>7c</sup> where it was pointed out that the  $\text{N}-\text{H}\cdots\text{O}$  hydrogen-bonded systems are more stable than the  $\text{O}-\text{H}\cdots\text{N}$  systems because of the greater proton affinity (PA) of nitrogen with respect to oxygen. The  $\text{R}_4$  substituent is able to lower the nitrogen PA if it is electron attractive, and the  $\text{R}_4$  substituent is able to increase the nitrogen PA if it is electron donating. For model systems investigated at the MP4/6-311++G(d,p) level,<sup>6</sup> for  $\text{R}_4 \approx \text{Li}$ , the only existing form is B ( $\text{N}-\text{H}\cdots\text{O}$ ) because the Li-substituent increases  $\text{N}-\text{PA}$ , and for the F-electron-withdrawing substituent, the tautomeric form A is more stable because the nitrogen PA decreases.

RAHBs belong to the broader class of  $\pi$ -conjugated systems; the study of crystal structures in which such systems appear was reported by Bertolasi et al.<sup>13</sup> Generally, the delocalization of  $\pi$ -electrons influences the properties of molecular species and greater aggregates of molecules in crystals, among them H-bonds. The influence of such delocalization on intermolecular hydrogen bonds and, vice versa, the influence of H-bonding formation on  $\pi$ -electron delocalization have not been investigated to such an extent as for intramolecular H-bonds. Hence, one of the aims of the present study is to consider the influence of  $\pi$ -electrons on the intermolecular H-bonding properties of pyrrole-2-carboxylic acid (PCA). In our previous report, we analyzed the molecular structures and vibrational spectra of PCA dimers using DFT results (the B3LYP/6-311+G(d) level of theory) as well as by applying the infrared and Raman spectroscopic studies.<sup>14</sup> Here, we analyze the crystal and molecular structure of PCA, showing that the X-ray crystal structure results are in excellent agreement with the previous theoretical and experimental spectroscopic results. To gain more insight into the influence of  $\pi$ -electrons on H-bonds, DFT and ab initio (MP2) calculations are performed on PCA and its dimers and on model complexes for which similar H-bonded patterns exist. Additionally, the more extended 6-311++G(d,p) basis set in comparison with that applied earlier<sup>14</sup> is used in this study to include diffusion and polarization functions on H-atoms, and this may be important for H-bonded systems investigated here. The Bader theory<sup>15</sup> is also applied to characterize the nature of interactions in terms of electron density and its Laplacian for bond and ring critical points.

### X-ray Measurement

Pyrrole-2-carboxylic acid was prepared by hydrolysis<sup>16</sup> of methyl pyrrole-2-carboxylate.<sup>14</sup> Block, colorless crystals of the investigated compound suitable for X-ray diffraction were obtained after recrystallization from methanol by slow evapo-

**TABLE 1: Crystallographic Data and Structure Refinement**

1	
formula	$\text{C}_5\text{H}_5\text{NO}_2$
M	111.10
crystal system	monoclinic
space group	$C2/c$
$a$ (Å)	13.34(2)
$b$ (Å)	5.075(5)
$c$ (Å)	15.15(2)
$\beta$ (deg)	99.21(7)
$V$ (Å <sup>3</sup> )	1012(2)
Z	8
$D_x$ (g cm <sup>-3</sup> )	1.458
$\mu$ (mm <sup>-1</sup> )	0.115
$T$ (K)	293(2)
$\lambda$ (Å)	0.71073
index ranges	$-16 \leq h \leq 16$ $-6 \leq k \leq 6$ $-18 \leq l \leq 18$
no. of data collected	4066
no. of unique data	995
$R_{\text{int}}$	0.0444
no. of $I > 2\sigma(I)$ data	899
no. of parameters	94
$R_1$ (all data)	0.0559
$wR_2$ (all data)	0.1152
$R_1 [I > 2\sigma(I)]$	0.0473
$wR_2 [I > 2\sigma(I)]$	0.1086
$\Delta\rho_{\text{min}}$ (e Å <sup>-3</sup> )	-0.167
$\Delta\rho_{\text{max}}$ (e Å <sup>-3</sup> )	0.176

ration of the solvent at room temperature. A single crystal mounted on glass fiber was used for measurement at room temperature on a KUMA KM4CCD diffractometer using an Mo  $K\alpha$  X-ray source. The unit cell dimensions were determined from 4066 reflections. The monitoring of two standard frames measured after each group of 50 frames showed no significant decays under X-ray irradiation. The structure was solved by direct methods using SHELXS-97<sup>17</sup> and refined by the full-matrix least-squares method on  $F^2$  using SHELXL-97.<sup>18</sup> After refinement with isotropic displacement parameters, refinement was continued with anisotropic displacement parameters for all non-hydrogen atoms. The positions of the hydrogen atoms were found on the difference Fourier map and were refined with isotropic thermal displacement parameters. A summary of crystallographic relevant data is given in Table 1.

The molecular geometry was calculated by PARST97<sup>19</sup> and PLATON.<sup>20</sup> Selected bond distances, angles, and geometries of hydrogen bonds are summarized in Tables 2 and 3. The drawings were made by PLATON.<sup>20</sup> Further experimental details, coordinates, and displacement parameters were placed in the Cambridge Structural Database (No. CCDC 221989).<sup>21</sup>

### Computational Details

The calculations were carried out with the Gaussian 98 set of codes.<sup>22</sup> The calculations of two conformers and three possible dimers of PCA were performed previously<sup>14</sup> at the B3LYP/6-311+G(d) level of theory. However, the optimized geometries were not analyzed in detail and hence are also presented here. In this study, the calculations for the same species have been performed at the B3LYP/6-311++G(d,p) and MP2/6-311++G(d,p) levels of theory. As before, for only DFT calculations,<sup>14</sup> the optimizations were performed here with symmetry constraints. For dimers of PCA, it was assumed that two molecules are linked through two equivalent hydrogen bonds (Chart 3) and that the dimers are centrosymmetric; that is, there is an inversion center between the linked species. For two cases, there are connections through the  $\text{O}-\text{H}\cdots\text{O}$  bonds

**TABLE 2: Bond Distances (angstroms) and Bond Angles (deg) for Non-hydrogen Atoms of the PCA Molecule; Estimated Standard Deviations Are Given in Parentheses**

Bonds	
O2—C1	1.315(2)
N1—C2	1.365(2)
N1—C5	1.351(3)
C1—C2	1.442(3)
C1—O1	1.230(2)
C2—C3	1.373(3)
C3—C4	1.400(3)
C5—C4	1.367(3)
Bond Angles	
C2—N1—C5	109.1(2)
O2—C1—C2	113.8(2)
O2—C1—O1	122.6(2)
C2—C1—O1	123.6(2)
N1—C2—C1	121.3(2)
N1—C2—C3	107.9(2)
C1—C2—C3	130.9(2)
C2—C3—C4	107.2(2)
N1—C5—C4	108.6(2)
C3—C4—C5	107.3(2)

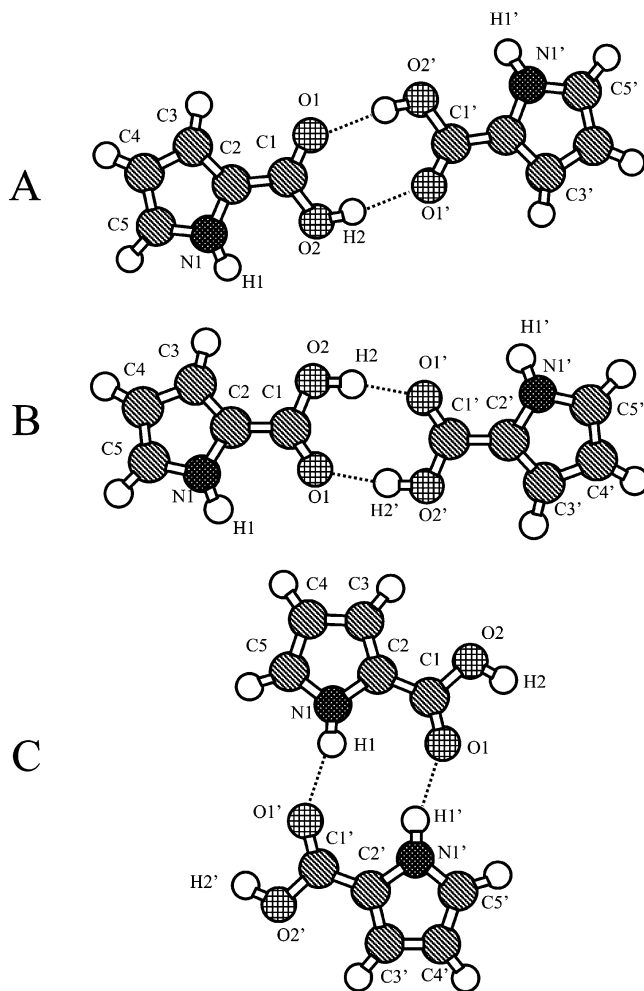
**TABLE 3: Possible Hydrogen Bonds and Their Geometries (Å, deg)**

donor—H	donor...acceptor	H...acceptor	donor—H...acceptor
N1—H1	N1...O1 (1)	H1...O1 (1)	N1—H1...O1 (1)
0.859(0.023)	2.997(0.003)	2.180(0.024)	158.76(2.12)
1.030		2.022	157.01 <sup>a</sup>
C5—H5	C5...O2 (2)	H5...O2 (2)	C5—H5...O2 (2)
0.979(0.026)	3.321(0.003)	2.513(0.025)	139.80(1.94)
1.080		2.437	138.27 <sup>a</sup>
O2—H2	O2...O1 (3)	H2...O1 (3)	O2—H2...O1 (3)
0.950(0.027)	2.647(0.003)	1.698(0.028)	176.32(2.74)
0.938		1.711	176.35 <sup>a</sup>

<sup>a</sup> Values normalized according to neutron diffraction corrections for H-atoms applied to X-ray results: Jeffrey, G. A.; Lewis, L. *Carbohydr. Res.* **1978**, *60*, 179. Taylor, R.; Kennard, O. *Acta Crystallogr.* **1983**, *B39*, 133. Equivalent positions: (0)  $x, y, z$ . (1)  $-x + 1/2, -y + 1/2 + 1, -z$ . (2)  $x + 1/2, +y + 1/2, +z$ . (3)  $-x, -y + 1, -z$ .

(A and B, Chart 3), and for one case it is through N—H...O (dimer C). Hence, for each of the dimers, there are pairs of geometrically equivalent molecules. All remaining parameters were optimized, including the O—H...O and N—H...O intermolecular contacts. Such an attitude is justified because, for the DFT calculations with symmetry constraints on the A, B, and C dimers, there are no imaginary frequencies for the optimized structures. Similar B3LYP/6-311++G(d,p) calculations have been performed on dimers without symmetry constraints, and the results are practically the same without imaginary frequencies. Additionally, the differences in bond lengths between equivalent molecules are less than  $10^{-5}$  Å, and the differences in energy between the structures optimized with symmetry constraints and those optimized without such constraints are less than  $3 \times 10^{-5}$  kcal/mol. Hence, the symmetry constraints were applied for the MP2/6-311++G(d,p) calculations. It is worth mentioning the difference between the A and B dimers; the first dimer consists of *s-trans* molecules; for the second dimer, the *s-cis* molecules are linked.

Additionally, the simple model systems were considered in this study, such as formic acid, ethanal amine, and ethanal imine. Calculations analogous to those for PCA were carried out for these model systems: full geometry optimizations for monomers and optimizations with symmetry constraints for dimers where the centrosymmetric moieties are linked through two equivalent H-bonds. The binding energies for the analyzed complexes have been computed as the difference between the total energy of

**CHART 3: Structures of the Possible Cyclic Dimers of Pyrrole-2-carboxylic Acid**

the complex and the energies of the isolated monomers and have been corrected for the basis set superposition error (BSSE) via the standard counterpoise method;<sup>23</sup> ZPE is not taken into account because the main goal of this study is to detect the influence of the  $\pi$ -electron delocalization on the geometrical and topological parameters. Because there are two equivalent H-bonds for the linked moieties within the complex, the H-bond energy is assumed to be half of the binding energy for the dimer.

For the systems analyzed, the “atoms in molecules” (AIM) theory of Bader<sup>15</sup> was applied to find bond and ring critical points<sup>24,25</sup> and to analyze them in terms of electron densities and their Laplacians. The AIM calculations were carried out using the “AIM2000” program.<sup>26</sup>

## Results and Discussion

**Crystal and Molecular Structure of PCA.** Table 2 presents the bond lengths and bond angles of the X-ray data for the PCA molecule. Figure 1 shows the molecular structure of PCA; the same designations of atoms are applied hereafter not only for crystal structure data but also for the ab initio and DFT results of the calculations of monomers and dimers of PCA. There are two conventional donating bonds for PCA: the O—H of the carboxylic group and N—H of the pyrrole ring and also the typical carbonyl accepting group. All of them may form hydrogen bonds in the crystal structure. Table 3 presents the shortest intermolecular contacts. Additionally, neutron diffraction corrections were performed for the bonds containing

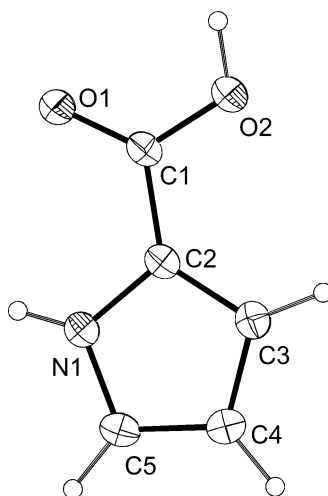


**Figure 1.** Molecular drawing of compound **1**. Displacement ellipsoids are drawn at the 30% probability level; the numbering of hydrogen atoms is the same as those atoms to which hydrogens are attached.

hydrogen atoms, and the results are also displayed in Table 3. It is well known that the accuracy of bond lengths for X-ray results is not as good as that for the bonds between non-hydrogen atoms. Hence, neutron diffraction corrections are often applied<sup>27,28</sup> as was done here for the PCA molecular structure.

One can see (Table 3) that there are the following kinds of hydrogen bonds. Two symmetry equivalent O2–H2···O1 bonds are between the carboxylic groups (see Figure 2). For the crystal structure of PCA, there are the centers of inversion within the eight-membered rings of the connected carboxylic groups as was similarly assumed for the calculations performed in this study. In the solid state, compounds containing carboxylic groups, especially the derivatives of benzoic acid, often form centrosymmetric dimers.<sup>29,30</sup> The C1–O2 and C1–O1 bond lengths for the PCA crystal structure are equal to 1.315 and 1.230 Å, respectively (Table 2), indicating that there is no meaningful equalization of the CO bonds. Thus, the disorder and/or the mesomeric effect for the carboxylic group of the PCA crystal structure are negligible even if they exist. These effects are often observed for the centrosymmetric dimers of carboxylic acids.<sup>29</sup> There are also two symmetry equivalent N1–H1···O1 hydrogen bonds (due to the inversion center) connecting the pyrrole rings with the carbonyl groups for the crystal structure

of PCA (Figure 2). One can see that the intermolecular connections presented above correspond to the B and C cyclic dimers (Chart 3) analyzed previously.<sup>14</sup> There are no A cyclic dimers because only the *s-cis* conformer exists in the analyzed crystal structure of PCA. Table 3 also presents the C5–H5···O2 interaction (Figure 2) that fulfills the geometrical criteria of the existence of hydrogen bonding, the H···O distance is less than the sum of the corresponding van der Waals radii, and the C–H···O angle is greater than 90°; the other C–H···O interactions of the crystal structure do not fulfill these geometrical criteria.

The crystal structure results mentioned above are in agreement with our previous studies<sup>14</sup> because, on the basis of spectroscopic investigations using both IR and Raman techniques, it was found that pyrrole-2-carboxylic acid exists in the solid state and in solution only in the *s-cis* form. Additionally, it was pointed out<sup>14</sup> that it forms cyclic dimers in the solid state and that the theoretically estimated frequencies (at the B3LYP/6-311+G(d) level) for the B and C dimers are very close to the experimental values. X-ray measurement confirms evidently the existence of these dimers and the lack of the A form (Chart 3).

It was also shown in our previous work<sup>14</sup> that for the A and B dimers one can point out the R<sub>2</sub><sup>2</sup>(8) motifs (H2–O2–C1=O1···H2'–O2'–C1'=O1'··· rings) according to the graph designation of Etter and Bernstein applied for the H-bonded patterns.<sup>30,31</sup> However, N–H···O bonds of the C dimer are assisted by two conjugated systems: the R<sub>2</sub><sup>2</sup>(10) ring, H1–N1–C2–C1=O1···H1'–N1'–C2'–C1'=O1'···, and the more extended R<sub>2</sub><sup>2</sup>(16) ring, H1–N1–C5–C4–C3–C2–C1=O1···H1'–N1'–C5'–C4'–C3'–C2'–C1'=O1'···. Such patterns exist in the crystal structure of PCA (Figure 2).

There are also C5–H5···O2 H-bonds (Table 3, Figure 2) for the PCA crystal structure. Hence, two equivalent O–H···O hydrogen bonds of the carboxylic groups are assisted through additional C–H···O and N–H···O contacts (Figure 2). Such a situation is similar to those existing for the crystal structure of benzoic acid and its *p*-substituted derivatives<sup>29</sup> where there are two C–H···O bonds between the oxygen atoms of the carboxylic groups and the C–H donors of the benzene ring. It is worth mentioning that all intermolecular contacts collected in Table 3 fulfill the geometrical criteria for the existence of hydrogen bonds.<sup>32</sup> All H···Y contacts are shorter than the

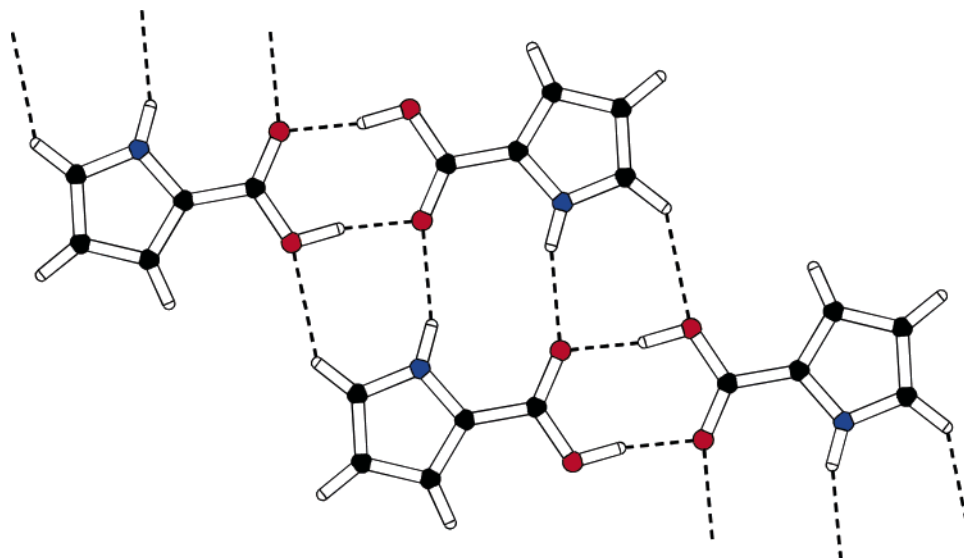


**Figure 2.** Scheme of hydrogen bonding between molecules.

**TABLE 4: Geometrical (in angstroms) and Energetic (in kcal/mol) Parameters of PCA and Its Dimers Calculated at the MP2/6-311++G(d,p) (Bold) and B3LYP/6-311++G(d,p) Levels of Theory and Compared with Experimental Solid-State X-ray Results**

	monomer, <i>s-trans</i>	monomer, <i>s-cis</i>	dimer A	dimer B	TS <sup>a</sup>	dimer C	exp.
C=O	1.209 <b>1.212</b>	1.216 <b>1.219</b>	1.231 <b>1.231</b>	1.238 <b>1.238</b>	1.271 <b>1.270</b>	1.225 <b>1.226</b>	1.230
C–O	1.371 <b>1.370</b>	1.356 <b>1.354</b>	1.332 <b>1.334</b>	1.322 <b>1.323</b>	1.282 <b>1.282</b>	1.354 <b>1.351</b>	1.315
O–H	0.968 <b>0.968</b>	0.968 <b>0.968</b>	1.001 <b>0.996</b>	1.000 <b>0.994</b>	1.198 <b>1.192</b>	0.968 <b>0.968</b>	0.950
H(O)···O			1.649 <b>1.657</b>	1.661 <b>1.670</b>	1.213 <b>1.207</b>		1.698
∠O–H···O			180.0 <b>179.7</b>	179.7 <b>179.6</b>	179.6 <b>179.7</b>		176.3
N–H	1.008 <b>1.011</b>	1.009 <b>1.012</b>	1.008 <b>1.011</b>	1.009 <b>1.012</b>	1.009 <b>1.012</b>	1.020 <b>1.020</b>	0.859
H(N)···O						1.880 <b>1.879</b>	2.180
∠N–H···O						163.7 <b>163.0</b>	158.8
EHB <sup>b</sup>			–8.5 <b>–7.9</b>	–8.0 <b>–7.4</b>		–5.9 <b>–6.3</b>	

<sup>a</sup> Transition state between A and B. <sup>b</sup> H-bond energy corrected for BSSE.

corresponding sum of the van der Waals radii, and all X–H···Y angles are greater than 90°.

**The Influence of Complexation of PCA on  $\pi$ -Electron Delocalization.** To explain in detail the influence of  $\pi$ -electron delocalization within dimers on the H-bonding strength, ab initio and DFT calculations have been performed here. The PCA monomers and dimers have been optimized at the B3LYP/6-311++G(d,p) and MP2/6-311++G(d,p) levels of theory with symmetry constraints as described in the previous section. Table 4 presents the geometrical and energetic results of these calculations. One can see that complexation causes equalization of the C=O and C–O bond lengths. This is greater for the A and B dimers than for the C dimer because, for the first two cases, the whole carboxylic group participates in the hydrogen bond interactions: the C=O carbonyl group and the O–H hydroxyl group. For the C dimer, there is practically no change in the C–O single bond length; there is only a slight shortening in comparison with the *s-cis* monomer. There is also a slight elongation of the OH proton-donating bonds for the A and B dimers. For the C dimer, the N–H bond is a donor; hence, elongation is observed. The H-bond energy decreases in the order from A to B and C. The H···O distances increase in the same order. One can see that the experimental X-ray data given in the last column are roughly in accordance with the theoretical results. The differences are probably connected with the influence of the lattice environmental effects that are not taken into account for calculations on A, B, and dimers. However, the greatest differences between calculations and experiment concern N–H, O–H bonds and H···O distances; this may be connected with the improper experimental lengths for the donating bonds (O–H and N–H). Neutron diffraction corrections were applied for them, but the effect of their elongation due to H-bond formation is not taken into account for such corrections. One can also see that there is the agreement between MP2 and DFT results (Table 4); the differences between C=O, C–O, and N–H bond lengths obtained within these methods are less than 0.003 Å, the differences between O–H bond lengths are less than 0.006 Å, the differences between H···O contacts are less than 0.01 Å, and the differences between the CC bond lengths (not presented in Table 4) of the pyrrole ring are of about 0.001 Å.

There are also results concerning the transition state (TS) between the A and B dimer conformations for the double proton-

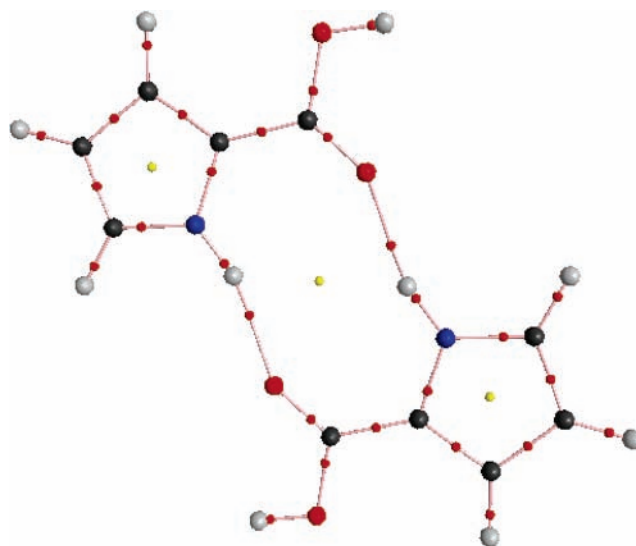


**Figure 3.** The molecular graph for the PCA dimer (C conformation of Chart 3); the attractors corresponding to atomic positions are given (big circles); small circles correspond to BCPs and RCPs (three RCPs, two of pyrrole rings and one created due to H-bond formation).

transfer reaction that may transfer one conformation into another one. There is the equalization of the C–O and C=O bonds for TS and approximately the central position of the hydrogen atom in the middle of the O···O distance. The geometrical parameters of the pyrrole ring do not change significantly due to the process of complexation; only slight changes (not greater than 0.001 Å) are observed. The greater changes are observed for the N–H bond only if it acts as a donor in hydrogen bonding for the C complex.

Recently, correlations between the characteristics of RCPs and the other parameters describing the H-bond strength were observed.<sup>33</sup> The electron density at RCP ( $\rho_{\text{RCP}}$ ) created due to H-bonding formation is greater for stronger H-bonds and was observed not only for intramolecular H-bonds<sup>6,9</sup> but also for intermolecular bonds.<sup>14</sup> Figure 3 shows the molecular graph of the C dimer with the critical points designated. One can see the ring critical point created due to the double hydrogen-bonding formation through the C=O and N–H bonds. For the dimers of PCA, the  $\rho_{\text{RCP}}$  values are greater for the A and B dimers and smaller for the C dimer (Table 5).

**TABLE 5: Topological Parameters (in au) of A, B, and C PC Dimers (Chart 3)<sup>a</sup>**

	A	B	TS <sup>b</sup>	C
$\rho_{\text{OH}}$	0.3163 <b>0.3171</b>	0.3187 <b>0.3195</b>	0.1736 <b>0.1734</b>	0.3599 <b>0.3544</b>
$\nabla^2\rho_{\text{OH}}$	-2.1906 <b>-2.2320</b>	-2.2145 <b>-2.2547</b>	-0.3246 <b>-0.3629</b>	-2.5211 <b>-2.4983</b>
$\rho_{\text{H(O)}\cdots\text{O}}$	0.0498 <b>0.0478</b>	0.0483 <b>0.0463</b>	0.1666 <b>0.1664</b>	
$\nabla^2\rho_{\text{H(O)}\cdots\text{O}}$	0.1408 <b>0.1422</b>	0.1396 <b>0.1409</b>	-0.2554 <b>-0.2870</b>	
$\rho_{\text{NH}}$	0.3402 <b>0.3336</b>	0.3394 <b>0.3329</b>	0.3397 <b>0.3331</b>	0.3280 <b>0.3240</b>
$\nabla^2\rho_{\text{NH}}$	-1.742 <b>-1.7778</b>	-1.7391 <b>-1.7733</b>	-1.7426 <b>-1.7775</b>	-1.7797 <b>-1.8344</b>
$\rho_{\text{H(N)}\cdots\text{O}}$				0.0263 <b>0.0259</b>
$\nabla^2\rho_{\text{H(N)}\cdots\text{O}}$				0.1056 <b>0.1065</b>
$\rho_{\text{RCP}}$	0.0081 <b>0.0083</b>	0.0081 <b>0.0084</b>	0.0104 <b>0.0110</b>	0.0030 <b>0.0032</b>
$\nabla^2\rho_{\text{RCP}}$	0.0317 <b>0.0325</b>	0.0318 <b>0.0325</b>	0.0485 <b>0.0507</b>	0.0131 <b>0.0143</b>

<sup>a</sup> The results were obtained at the MP2/6-311++G(d,p) (bold) and B3LYP/6-311++G(d,p) levels of theory. <sup>b</sup> Transition state between A and B.

As was mentioned, there are differences between the A and B dimers, on one hand, and the C dimer, on the other hand; the geometrical changes due to the complexation are greater for A and B than for C. It seems that  $\pi$ -electron delocalization is greater for former systems than for the latter one. The explanation is as follows: the O–H $\cdots$ O hydrogen bond is stronger than the N–H $\cdots$ O bond, and hence the former makes greater geometrical changes (see Table 4); another explanation is connected with the features of resonance-assisted hydrogen bonds (RAHBs).<sup>7c</sup> The A and B dimers may be treated as intermolecular RAHBs; for both of them, one can expect the contribution of the other form obtained after the double proton-transfer process. In other words, for the system with RAHB, the corresponding wave function is the linear combination of the wave functions of the tautomeric forms.<sup>7c</sup> Hence, the wave function of the A dimer contains also the contribution of the pure B tautomeric form and vice versa; the wave function of the B dimer contains the contribution of the pure A tautomeric form. For the C dimer, there is no other similar tautomeric form obtainable after the double proton-transfer process.

**The  $\pi$ -Electron Delocalization for Other Species Related to PCA.** Calculations concerning the formic acid dimer (FAD) have been performed here for comparison with the results of PCA because for FAD the double connection through O–H $\cdots$ O bonds is observed similarly as for the A and B dimers of PCA. Table 6 collects the geometrical, topological, and energetic results for monomers and dimers of formic acid. The results corresponding to the transition state are also given. A lot of papers reported the results on FAD and the double proton transfer for it.<sup>34–37</sup> The results collected here are given only for comparison with PCA and were obtained at the corresponding levels of theory (the MP2 and B3LYP methods, the 6-311++G(d,p) basis set). One can see that there are weaker H-bonds for FAD than for the A and B dimers of PCA and that they are a little stronger or comparable with the C dimer. At least two most often applied parameters of H-bond strength support it: the H-bond energy and the electron density at H $\cdots$ O BCP –  $\rho_{\text{H}\cdots\text{O}}$ . If we take into account the MP2 results, there are the following H-bond energies for the A, B, FAD, and C complexes: -7.9, -7.4, -6.6, and -6.3 kcal/mol, respectively. The following electron densities at the H $\cdots$ O BCPs

**TABLE 6: Geometrical (in angstroms), Energetic (in kcal/mol), and Topological (in au) Parameters of the Formic Acid Monomer and Dimer Calculated at the MP2/6-311++G(d,p) (Bold) and B3LYP/6-311++G(d,p) Levels of Theory**

	monomer	dimer	TS <sup>a</sup>
C=O	1.199 1.205	1.219 1.221	1.261 1.264
C–O	1.346 1.348	1.313 1.319	1.261 1.264
O–H	0.971 0.969	0.998 0.990	1.208 1.201
H $\cdots$ O		1.702 1.726	1.210 1.201
O–H $\cdots$ O		176.5 177.9	180.0 179.9
$E_{\text{HB}}^b$		-7.4 -6.6	
$\rho_{\text{OH}}$	0.3573 0.3540	0.3225 0.3265	0.1696 0.1701
$\nabla^2\rho_{\text{OH}}$	-2.494 -2.493	-2.254 -2.326	-0.2851 -0.3243
$\rho_{\text{H(O)}\cdots\text{O}}$		0.0435 0.0400	0.1689 0.1698
$\nabla^2\rho_{\text{H(O)}\cdots\text{O}}$		0.1304 0.1292	-0.2783 -0.3209
$\rho_{\text{RCP}}$		0.0074 0.0076	0.0099 0.0106
$\nabla^2\rho_{\text{RCP}}$		0.0293 0.0297	0.0475 0.0505

<sup>a</sup> Transition state between A and B. <sup>b</sup> H-bond energy corrected for BSSE.

are given in the same order: 0.0478, 0.0463, 0.0400, and 0.0259 au, respectively. There are comparable values of about 0.008 au for electron densities at the RCPs for A, B, and FAD and a much lower value of 0.003 au for the C dimer. Similarly, the H $\cdots$ O distances show that the C dimer is linked through weaker H-bonds than the remaining A, B, and FAD complexes.

We have found previously<sup>14</sup> on the basis of IR, Raman, and theoretical investigations that PCA exists in solution and in the solid state in only one *s-cis* conformation and that probably only the B and C dimers exist in crystals. This conclusion is nicely confirmed here by X-ray crystal structure determination (Figure 2). It was also pointed out previously that the *s-cis* conformation is energetically more stable than the *s-trans* conformation.<sup>14</sup> Hence, the process of transformation of the *s-cis* form into *s-trans* is investigated here. Figure 4 shows the dependence between the energy of the PCA monomer and the angle between the planes of the pyrrole ring and of the carboxylic group. Different levels of theory are applied. The more stable *s-cis* conformation is assumed here as the reference (zero energy level – Figure 4). One can see that the barrier height for the transformation of the *s-cis* conformer into the *s-trans* conformer amounts to 11.3 kcal/mol (the MP2/6-311++G(d,p) level of theory). B3LYP and HF calculations show only a slightly higher barrier height. The change of *s-cis* into *s-trans* is also possible through the double proton-transfer reaction, the transfer of B dimers into A dimers. The potential barrier height for this process is equal to 7.6 kcal/mol calculated at the MP2/6-311++G(d,p) level (6.7 kcal/mol at the B3LYP/6-311++G(d,p) level). This may be the reason only the *s-cis* form exists in solution as well as in the solid state. For comparison, the potential barrier height for the double proton transfer for FAD amounts to 8.8 and 7.3 kcal/mol for the MP2 and DFT methods, respectively, but in such a case there is no change in the conformation due to the double proton transfer. It was pointed out that the environmental effects in crystals may influence the decrease in barrier height for the double proton-

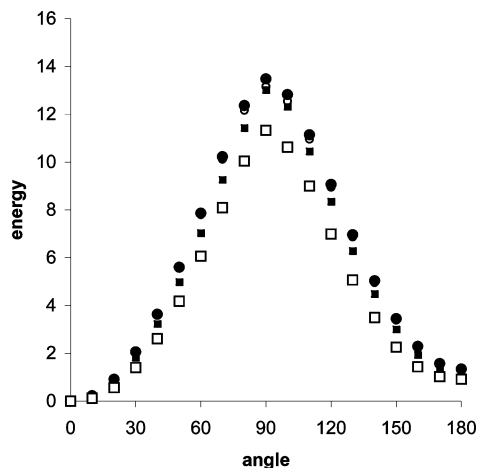


**Figure 4.** The relationship between the energy of PCA (kcal/mol) and the rotation angle (pyrrole ring – carboxylic group); full circles are the HF/6-31G\* results, empty circles are the HF/6-311+G\* results, full squares are the B3LYP/6-311++G(d,p) results, and empty squares are the MP2/6-311++G(d,p) results.

**TABLE 7: Geometrical (in angstroms), Energetic (in kcal/mol), and Topological (in au) Parameters of Ethanal Amine and Ethanal Imine Monomers and Dimers, Calculated at the MP2/6-311++G(d,p) (Bold) and B3LYP/6-311++G(d,p) Levels of Theory**

	ethanal imine – monomer	ethanal imine – dimer	ethanal amine – monomer	ethanal amine – dimer
N=C (or N–C)	1.267	1.267	1.449	1.445
	<b>1.281</b>	<b>1.280</b>	<b>1.451</b>	<b>1.448</b>
C–C	1.514	1.511	1.507	1.504
	<b>1.513</b>	<b>1.511</b>	<b>1.509</b>	<b>1.506</b>
C=O	1.206	1.208	1.206	1.208
	<b>1.216</b>	<b>1.217</b>	<b>1.215</b>	<b>1.216</b>
N–H	1.029	1.028	1.015	1.016
	<b>1.030</b>	<b>1.029</b>	<b>1.015</b>	<b>1.016</b>
H···O		2.237		2.171
		<b>2.260</b>		<b>2.161</b>
N–H···O		159.8		161.0
		<b>162.7</b>		<b>161.8</b>
$E_{\text{HB}}$		-1.1		-1.9
		<b>-1.6</b>		<b>-2.5</b>
$\rho_{\text{NH}}$	0.3303	0.3302	0.3361	0.3358
	<b>0.3267</b>	<b>0.3271</b>	<b>0.3334</b>	<b>0.3335</b>
$\nabla^2\rho_{\text{NH}}$	-1.493	-1.558	-1.545	-1.589
	<b>-1.514</b>	<b>-1.570</b>	<b>-1.583</b>	<b>-1.628</b>
$\rho_{\text{H(N)···O}}$		0.0117		0.0138
		<b>0.0111</b>		<b>0.0140</b>
$\nabla^2\rho_{\text{H(N)···O}}$		0.0447		0.0538
		<b>0.0429</b>		<b>0.0558</b>
$\rho_{\text{RCP}}$		0.0036		0.0023
		<b>0.0041</b>		<b>0.0025</b>
$\nabla^2\rho_{\text{RCP}}$		0.0134		0.0103
		<b>0.0152</b>		<b>0.0113</b>

transfer reaction for benzoic acid and its simple derivatives.<sup>38,39</sup> However, it seems that such a decrease does not take place in the case of the solid-state PCA.

The weakest hydrogen-bonding interactions for PCA are revealed for the C dimers. However, these interactions may be also classified as H-bonds of medium strength. To gain more insight into the influence of  $\pi$ -electron delocalization of pyrrole rings on the strength of H-bonds for the C dimer, calculations of simple model systems were performed here. Table 8 shows the B3LYP and MP2 results for the ethanal imine and ethanal amine monomers and dimers connected through N–H···O bonds, similarly to that for the C dimer. The single MP2 level H-bond energy for the ethanal imine dimer is equal to 1.6 kcal/

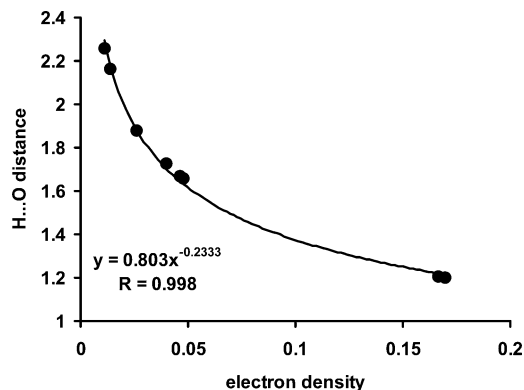


**Figure 5.** The relationship between the H···O intermolecular distance (Å) and the electron density at H···O BCP.

mol, while for ethanal amine it amounts to 2.5 kcal/mol. The existence of stronger H-bonds for the latter is confirmed by AIM calculations because the electron density at H···O BCP is equal to 0.0111 and 0.0140 au for ethanal imine and ethanal amine, respectively. One could expect the reverse situation due to the  $\pi$ -electron delocalization for the N=C–C=O imine system. However, only  $\rho_{\text{RCP}}$  values suggest rather stronger H-bonds for ethanal imine ( $\rho_{\text{RCP}} = 0.0041$  au), while for amine it is equal to 0.0025 au. It seems that  $\rho_{\text{RCP}}$  is not always as good of a measure of H-bond strength as other parameters such as H-bond energies,  $\rho_{\text{H···O}}$  electron densities, and H···O distances, which clearly show that for amine dimers H-bonds are stronger. Figure 5 shows the relationship between the H···O intermolecular distance and the  $\rho_{\text{H···O}}$  value for all systems investigated here such as dimers of PCA and model complexes. This is a good correlation with the correlation coefficient of 0.998. It indicates that both H···O and electron density are good descriptors of H-bond strength. The similar correlations between the geometrical and topological parameters have been observed previously for different samples of H-bonded systems.<sup>40</sup>

The data of Table 7 show that the existence of  $\pi$ -electrons does not enlarge the H-bond strength. There is no difference between the geometries of monomers and dimers. Hence, one can see that the process of complexation does not influence the  $\pi$ -electron delocalization for connected species. A similar situation was observed earlier for methyl-hydrazine, methylene-hydrazine, and 3-hydrazono-propen-1-ol complexes with formaldehyde (B3LYP/6-311++G(d,p) and MP2/6-311++G(d,p) calculations).<sup>41</sup> The special feature of pyrrole rings is revealed in these results because for similar connections of the C dimer there are much stronger H-bonds than for ethanal imine and ethanal amine dimers. The elongation of the proton-donating N–H bond length from 1.012 to 1.020 Å and also of the C=O bond from 1.219 to 1.226 Å due to the complexation of *s-cis* moieties into the C dimer is observed (MP2 method). This means that in such a case  $\pi$ -electron delocalization due to H-bond formation takes place but it is not as meaningful as for A and B dimers where RAHBs exist.

There is the following explanation that the geometries of ethanal imine and ethanal amine practically do not change due to the complexation. Particularly for ethanal imine, one may expect the greater  $\pi$ -electron delocalization leads to H-bond formation and hence the greater changes of the geometrical parameters. However, there are not tautomeric forms for dimers of ethanal imine and ethanal amine obtainable due to proton-transfer processes, and hence RAHBs supported by  $\pi$ -electron delocalization do not exist.

## Summary

We have shown the influence of pyrrole rings on the geometry of pyrrole-2-carboxylic acid molecules for different kinds of dimers (Chart 3). The H-bonds for PCA are stronger than those existing for model related systems. The strongest H-bonds were detected in this study for the A and B dimers; H-bonds for the C dimer are weaker. It is confirmed by energetic, geometric, and topological (AIM) results. H-bonds for A and B are also stronger than those of the formic acid dimer. The  $\pi$ -electron delocalization influences significantly the parameters of PCA molecules and the strength of the H-bonds.

The results of the X-ray crystal structure determination of PCA are in agreement with our previous IR and NMR investigations. Both the B and the C dimers exist in a crystal structure; however, A does not exist in a crystal structure as was predicted previously using experimental and theoretical techniques.<sup>14</sup>

There are other findings of this study connected with features of the resonance-assisted hydrogen bonds. For the A and B dimers of PCA as well as for the formic acid dimer, one can detect intermolecular RAHBs. For these systems, the real molecular structures may be treated as mixtures of tautomeric forms, and the process of  $\pi$ -electron delocalization supports their effective mixing. For dimers of ethanal imine and ethanal amine, there are not tautomeric forms obtainable due to the proton-transfer process, and hence H-bonds are not assisted through the resonance; similarly, for the C dimer, hydrogen bonds are not supported by the existence of effectively mixing tautomeric forms.

**Acknowledgment.** Support for this research is provided by grant No. 505/675 2004 (University of Łódź), NSF CREST No. 9805465, NSF EPSCoR 94475601, and ONR Grant N00014-98-1-0592.

## References and Notes

- (1) Jeffrey, G. A.; Saenger, W. *Hydrogen Bonding in Biological Structures*; Springer-Verlag: Berlin, 1991.
- (2) Allen, F. H.; Motherwell, W. D. S.; Raithby, P. R.; Shields, G. P.; Taylor, R. *New J. Chem.* **1999**, 23, 25.
- (3) Desiraju, G. R. *Crystal Engineering—The Design of Organic Solids*; Elsevier: Amsterdam, 1989.
- (4) Jeffrey, G. A. *An Introduction to Hydrogen Bonding*; Oxford University Press: New York, 1997.
- (5) Desiraju, G. R.; Steiner, T. *The Weak Hydrogen Bond in Structural Chemistry and Biology*; Oxford University Press, Inc.: New York, 1999.
- (6) Rybarczyk-Pirek, A. J.; Grabowski, S. J.; Małeczka, M.; Nawrot-Modranka, J. *J. Phys. Chem. A* **2002**, 106, 11956.
- (7) (a) Gilli, G.; Bellucci, F.; Ferretti, V.; Bertolasi, V. *J. Am. Chem. Soc.* **1989**, 111, 1023. (b) Bertolasi, V.; Gilli, P.; Ferretti, V.; Gilli, G. *J. Am. Chem. Soc.* **1991**, 113, 4917. (c) Gilli, P.; Bertolasi, V.; Ferretti, V.; Gilli, G. *J. Am. Chem. Soc.* **1994**, 116, 909. (d) Gilli, P.; Bertolasi, V.; Ferretti, V.; Gilli, G. *J. Am. Chem. Soc.* **2000**, 122, 10405. (e) Gilli, P.; Bertolasi, V.; Pretto, L.; Lyčka, A.; Gilli, G. *J. Am. Chem. Soc.* **2002**, 124, 13554. (f) Gilli, P.; Bertolasi, V.; Pretto, L.; Ferretti, V.; Gilli, G. *J. Am. Chem. Soc.* **2004**, 126, 3845.
- (8) Madsen, G. K. H.; Iversen, B. B.; Larsen, F. K.; Kapon, M.; Reisner, G. M.; Herbstein, F. H. *J. Am. Chem. Soc.* **1998**, 120, 10040.

- (9) Wojtulewski, S.; Grabowski, S. J. *Chem. Phys. Lett.* **2003**, 378, 388.
- (10) Grabowski, S. J. *J. Mol. Struct.* **2001**, 562, 137.
- (11) (a) González, L.; Mó, O.; Yáñez, M. *J. Org. Chem.* **1999**, 64, 2314. (b) Sanz, P.; Yáñez, M.; Mó, O. *J. Phys. Chem. A* **2002**, 106, 4661.
- (12) Rybarczyk, A. J.; Małeczka, M.; Grabowski, S. J.; Nawrot-Modranka, J. *Acta Crystallogr., Sect. C* **2002**, 58, 405.
- (13) Bertolasi, V.; Gilli, P.; Ferretti, V.; Gilli, G. *Acta Crystallogr., Sect. B* **1995**, 51, 1004.
- (14) Dubis, A.; Grabowski, S. J.; Romanowska, D. B.; Misiaszek, T.; Leszczynski, J. *J. Phys. Chem. A* **2002**, 106, 10613.
- (15) Bader, R. F. W. *Atoms in Molecules. A Quantum Theory*; Oxford University Press: New York, 1990.
- (16) Anderson, H. J.; Hopkins, L. C. *Can. J. Chem.* **1964**, 42, 1279.
- (17) Sheldrick, G. M. *SHELXS*, Program for Crystal Structure Solution; University of Göttingen: Germany, 1997.
- (18) Sheldrick, G. M. *SHELXL*, Program for Refinement of Crystal Structures; University of Göttingen: Germany, 1997.
- (19) Nardelli, M. *J. Appl. Crystallogr.* **1996**, 29, 296.
- (20) Spek, A. L. *PLATON*, Molecular Geometry Program; University of Utrecht: The Netherlands, 1998.
- (21) *Cambridge Structural Database System*; Cambridge Crystallographic Data Centre: Cambridge, U.K., 2003.
- (22) Frisch, M. J.; Trucks, G. W.; Schlegel, H. B.; Scuseria, G. E.; Robb, M. A.; Cheeseman, J. R.; Zakrzewski, V. G.; Montgomery, J. A.; Stratmann, R. E.; Burant, J. C.; Dapprich, S.; Millam, J. M.; Daniels, A. D.; Kudin, K. N.; Strain, M. C.; Farkas, O.; Tomasi, J.; Barone, V.; Cossi, M.; Cammi, R.; Mennucci, B.; Pomelli, C.; Adamo, C.; Clifford, S.; Ochterski, J.; Petersson, G. A.; Ayala, P. Y.; Cui, Q.; Morokuma, K.; Malick, D. K.; Rabuck, A. D.; Raghavachari, K.; Foresman, J. B.; Cioslowski, J.; Ortiz, J. V.; Stefanov, B. B.; Liu, G.; Liashenko, A.; Piskorz, P.; Komaromi, I.; Gomperts, R.; Martin, L. R.; Fox, D. J.; Keith, T.; Al-Laham, M. A.; Peng, C. Y.; Nanayakkara, A.; Gonzalez, G.; Challacombe, M.; Gill, P. M. W.; Johnson, B.; Chen, W.; Wong, M. W.; Andres, J. L.; Gonzalez, C.; Head-Gordon, M.; Replogle, E. S.; Pople, J. A. *Gaussian 98*, revision A.6; Gaussian, Inc.: Pittsburgh, PA, 1998.
- (23) Boys, S. F.; Bernardi, F. *Mol. Phys.* **1970**, 19, 553.
- (24) Carrol, M. T.; Chang, C.; Bader, R. F. W. *Mol. Phys.* **1988**, 63, 387.
- (25) Carrol, M. T.; Bader, R. F. W. *Mol. Phys.* **1988**, 65, 695.
- (26) AIM2000 designed by Friedrich Biegler-König, University of Applied Sciences, Bielefeld, Germany.
- (27) Jeffrey, G. A.; Lewis, L. *Carbohydr. Res.* **1978**, 60, 179.
- (28) Taylor, R.; Kennard, O. *Acta Crystallogr.* **1983**, B39, 133.
- (29) Leiserowitz, L. *Acta Crystallogr., Sect. B* **1976**, 32, 775.
- (30) Bernstein, J.; Etter, M. C.; Leiserowitz, L. The Role of Hydrogen Bonding in Molecular Assemblies. In *Structure Correlation*; Bürgi, H.-B., Dunitz, J. D., Eds.; VCH: Weinheim, 1994.
- (31) Etter, M. C. *Acc. Chem. Res.* **1990**, 23, 120.
- (32) Taylor, R.; Kennard, O. *J. Am. Chem. Soc.* **1982**, 104, 5063.
- (33) Grabowski, S. J. *Monatsh. Chem.* **2002**, 133, 1373.
- (34) Chojnacki, H.; Andzelm, J. W.; Nguyen, D. T.; Sokalski, W. A. *Comput. Chem.* **1995**, 19, 181.
- (35) Kim, Y. *J. Am. Chem. Soc.* **1996**, 118, 1522.
- (36) Miura, S.; Tuckerman, M. E.; Klein, M. L. *J. Chem. Phys.* **1998**, 109, 5290.
- (37) Ushiyama, H.; Takatsuka, K. *J. Chem. Phys.* **2001**, 115, 5903.
- (38) Grabowski, S. J.; Krygowski, T. M. *Chem. Phys. Lett.* **1988**, 151, 425.
- (39) Grabowski, S. J.; Krygowski, T. M. *Chem. Phys. Lett.* **1999**, 305, 247.
- (40) (a) Alkorta, I.; Rozas, I.; Elguero, J. *Struct. Chem.* **1998**, 9, 243. (b) Alkorta, I.; Barrios, L.; Rozas, I.; Elguero, J. *J. Mol. Struct. (THEOCHEM)* **2000**, 496, 131. (c) Alkorta, I.; Elguero, J.; Mó, O.; Yáñez, M.; Del Bene, J. E. *J. Phys. Chem. A* **2002**, 106, 9325. (d) Pacios, L. F. *J. Phys. Chem. A* **2004**, 108, 1177.
- (41) Rybarczyk-Pirek, A. J.; Grabowski, S. J.; Nawrot-Modranka, J. *J. Phys. Chem. A* **2003**, 107, 9232.